CROATICA CHEMICA ACTA CCACAA **72** (2–3) 351–363 (1999)

ISSN-0011-1643
CCA-2582 *Original Scientific Paper*

Crystal and Molecular Structure of Secoisolariciresinol*

Marco Milanesio,[a] *Davide Viterbo,*[a,**] *Sunil K. Chattopadhyay,*[b] *Manish Kulshrestha,*[b] *and Giovanni Appendino*[c]

[a] *Dipartimento di Chimica IFM, Università, Via P. Giuria 7, I-10125 Torino, and Dipartimento di Scienze e Tecnologie Avanzate, Università del Piemonte Orientale »A. Avogadro«, Corso T. Borsalino 54, I-15100 Alessandria, Italy*

[b] *Central Institute of Medicinal and Aromatic Plants, PO CIMAP, Lucknow, 226 015 India*

[c] *Dipartimento di Scienza e Tecnologia del Farmaco, Università, Via P. Giuria 9, I-10125 Torino, Italy*

Received November 9, 1998; revised January 27, 1999; accepted February 2, 1999

The *R,R*-2,3-bis[(4-hydroxy-3-methoxyphenyl)methyl]-1,4-butandiol lignan secoisolariciresinol (**1**) is a constituent of Gymnosperms used in the treatment of benign prostatic hyperplasya. The results of crystallographic and *ab initio* theoretical studies are reported and discussed. In the crystal, the molecule of (**1**) assumes a clustered conformation, characterized by the facing of the two phenyl rings. This geometry is stabilized by the formation of a network of hydrogen bonds. Theoretical calculations indicate that: *i)* the intramolecular hydrogen bond O1–H1 ··· O1' is the major factor dictating the facing of the two phenyl groups, while intermolecular hydrogen bonds and crystal packing have smaller effects; *ii)* the 1–4O ··· O non-bonded interactions in the vanillyl groups are important in determining the most stable conformation; *iii)* calculations with two explicit water molecules in the model give a good simulation of the local effects of a water solvent and indicate that (**1**) probably assumes a clustered conformation also in polar solvents.

Key words: secoisolariciresinol, lignan, structure, bioactivity, *ab initio* calculations.

---

* Dedicated to Professor Boris Kamenar on the occasion of his 70th birthday.

** Author to whom correspondence should be addressed.

INTRODUCTION

The 1,4-butandiol lignan secoisolariciresinol (**1**) is a typical heartwood constituent of Gymnosperms,[1] also reported, mainly in ester and glucosidic form, in many Angiosperms.[2] Interest in this lignan was sparkled by the discovery of its binding to human SHBG (sex hormone binding globulin), an allosteric protein involved in the genesis of benign prostatic hyperplasya (BHP).[3] (**1**) is in fact considered one of the main active constituents of the roots of stinging nettle (*Urtica dioica* L.), whose extracts are used for the treatment of BHP.[3] The roots contain (**1**) in glucosidic form, from which the free diol is then released by intestinal microbial transformation. (**1**) is flexible, and its active conformation is not known; the activity of its conformationally constrained semisynthetic analogue (**2**) suggests however that a clustered conformation with a synclinal relationship between the two hydroxymethyl groups is relevant to bioactivity.[3]

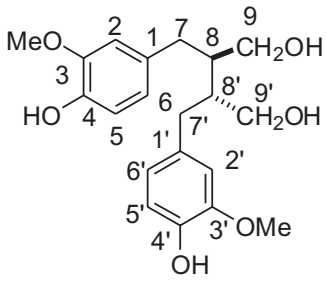

1

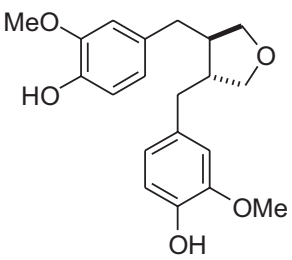

2

The absolute configuration of (**1**) has been established to be *R,R* by chemical correlation studies.[4]

We report here a crystallographic study showing that the suggested conformational features of (**1**) are indeed found in the solid state. *Ab initio* theoretical calculations were also carried out in order to analyze the factors contributing to the stability of this conformation in the solid state and in solution.

EXPERIMENTAL

Crystals of secoisolariciresinol (**1**) suitable for X-ray analysis were obtained by evaporation of a benzene/acetone solution. Crystallographic data and details of data collection and refinement are given in Table I. Data reduction was carried out by the Siemens P3/PC program[5] and only Lorentz and polarization corrections

were performed. The structure was solved by direct methods using the SIR92 program[6] and refined using the SHELXTL/IRIS[7] and SHELXL97[8] programs. The refinement was done by the least-squares full matrix method, with anisotropic displacement parameters for all non-hydrogen atoms. Hydrogen atoms were located in the calculated positions and treated as riding atoms during the refine-

TABLE I

Crystal data, structure solution and refinement for secoisolariciresinol (**1**)

Crystal data	
Empirical formula	$C_{20}H_{26}O_6$
Formula weight	362.41
Crystal system	Orthorhombic
Space group	$P2_12_12_1$
Unit cell dimensions	a = 7.439(1) Å
	b = 12.803(2) Å
	c = 19.716(3) Å
Volume	1877.8(6) Å^3
Z	4
Density (calculated)	1.282 g/cm^3
Absorption coefficient	0.094 mm^{-1}
F(000)	776
Crystal size	0.5 × 0.5 × 0.45 mm^3
Data collection	
Diffractometer	Siemens R3m/v
Radiation	Mo-Kα (λ = 0.71069 Å)
	graphite monochromator
Temperature	room
θ range for data collection	1.90 to 29.98°
h k l limits	0→10, 0→17, 0→27
Reflections collected	3104
Reflections observed [$I>2\sigma(I)$]	1951
Refinement	
Refinement method	Full-matrix least-squares on F^2
Data / parameters	3036 / 235
Goodness-of-fit on F^2	1.028
Final R indices [$I>2\sigma(I)$]	$R1$ = 0.0522, $wR2$ = 0.1120
R indices (all data)	$R1$ = 0.0940, $wR2$ = 0.1303
Largest $\Delta\rho$ peak and hole	0.165 and –0.206 e Å^{-3}

ment. Final atomic coordinates and equivalent isotropic temperature factors are listed in Table II.*

TABLE II

Atomic coordinates (x, y, $z \times 10^4$) and equivalent isotropic displacement parameters ($U_{eq} \times 10^3$ / Å^2) for (**1**)

Atom	x	y	z	U_{eq}
C(1)	10827(4)	–935(2)	10289(2)	42(1)
C(2)	10805(4)	–85(2)	10735(1)	42(1)
C(3)	10175(4)	–192(2)	11386(1)	41(1)
C(4)	9525(5)	–1155(2)	11614(2)	47(1)
C(5)	9567(5)	–1997(2)	11185(2)	52(1)
C(6)	10214(5)	–1887(2)	10528(2)	51(1)
C(7)	11524(5)	–800(3)	9578(2)	50(1)
C(8)	10411(4)	–39(2)	9144(1)	38(1)
C(9)	11541(5)	315(2)	8543(2)	52(1)
C(10)	10846(6)	1569(3)	11700(2)	69(1)
O(1)	10724(4)	1107(2)	8146(1)	59(1)
O(2)	8862(4)	–1268(2)	12256(1)	62(1)
O(3)	10090(4)	581(2)	11862(1)	59(1)
C(1')	6705(4)	722(2)	9709(1)	41(1)
C(2')	6073(4)	84(2)	10230(1)	43(1)
C(3')	5811(4)	464(2)	10876(1)	39(1)
C(4')	6187(4)	1506(2)	11017(1)	43(1)
C(5')	6852(5)	2144(2)	10512(2)	51(1)
C(6')	7101(5)	1747(3)	9860(2)	50(1)
C(7')	7009(4)	277(3)	9006(1)	47(1)
C(8')	8552(4)	–511(2)	8970(1)	36(1)
C(9')	8487(5)	–1117(2)	8304(1)	45(1)
C(10')	4827(5)	–1182(2)	11329(2)	51(1)
O(1')	8424(3)	–393(2)	7749(1)	50(1)
O(2')	5922(4)	1834(2)	11676(1)	55(1)
O(3')	5190(3)	–95(2)	11420(1)	50(1)

U_{eq} is defined as one third of the trace of the orthogonalized $\boldsymbol{U}_{ij}$ tensor.

* Crystallographic data for the structure reported have been deposited with the Cambridge Crystallographic Data Centre (No. 109442). Deposited data can be obtained from the CCDC Technical Editors by e-mail request at deposit@ccdc.cam.ac.uk (excluding structure factors which are available from the Editorial Office of CCA).

Ab initio Hartree-Fock (HF) and Density Fuctional (DFT) SCF-MO calculations on (**1**) were performed using the Gaussian94 program.[9] The initial geometry was the one obtained from the X-ray analysis and the geometry optimization was carried out, at HF level, using 6–31G(d,p) and/or 6–31G(d) basis sets.[10] Single point Becke-3LYP DFT calculations were performed on the above optimized geometries in order to obtain more accurate estimates of their relative energy.

The graphic analysis was mainly performed using the MOLDRAW program,[11] while the retrieval of the related structures was carried out using the Cambridge Structural Database.[12]

RESULTS AND DISCUSSION

The X-ray molecular structure is shown in Figure 1, together with the adopted atomic labeling scheme; the interatomic distances, bond angles and selected torsion angles are listed in Table III.

The molecule adopts a tweezers shape with the two vanillyl (*m*-methoxy-*p*-hydroxyphenyl) moieties acting as the arms, and a pseudo-twofold axis passing through the mid point of bond C8–C8' and parallel to the arms. The

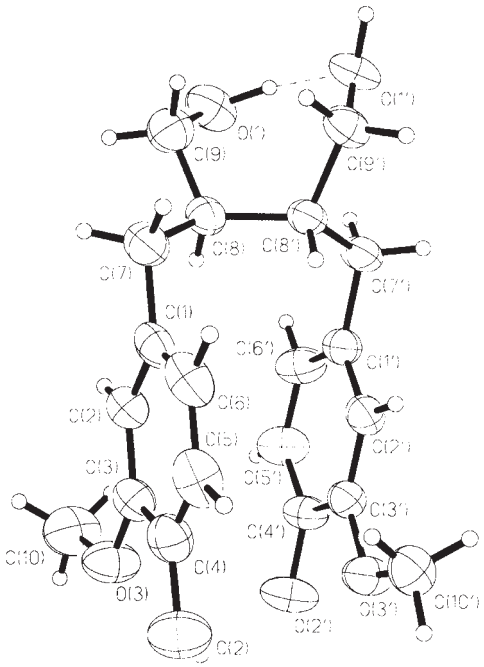

Figure 1. Drawing of the molecular structure of compound (**1**) showing the adopted labeling scheme. Displacement ellipsoids are drawn at the 30% probability level.

TABLE III

Bond lengths / Å, angles / ° and selected torsion angles / ° for (**1**)

Bond lengths / Å			
C(1)–C(6)	1.385(4)	C(1')–C(6')	1.378(5)
C(1)–C(2)	1.399(4)	C(1')–C(2')	1.394(4)
C(1)–C(7)	1.504(4)	C(1')–C(7')	1.516(4)
C(2)–C(3)	1.374(4)	C(2')–C(3')	1.378(4)
C(3)–O(3)	1.366(3)	C(3')–O(3')	1.370(3)
C(3)–C(4)	1.399(4)	C(3')–C(4')	1.391(4)
C(4)–O(2)	1.365(4)	C(4')–O(2')	1.380(3)
C(4)–C(5)	1.370(4)	C(4')–C(5')	1.379(4)
C(5)–C(6)	1.389(5)	C(5')–C(6')	1.395(4)
C(7)–C(8)	1.540(4)	C(7')–C(8')	1.530(4)
C(8)–C(9)	1.521(4)	C(8')–C(9')	1.525(4)
C(8)–C(8')	1.548(4)	C(9')–O(1')	1.434(3)
C(9)–O(1)	1.417(4)	C(10')–O(3')	1.429(4)
C(10)–O(3)	1.422(4)		
Bond angles / °			
C(6)–C(1)–C(2)	117.9(3)	C(6')–C(1')–C(2')	118.1(3)
C(6)–C(1)–C(7)	122.1(3)	C(6')–C(1')–C(7')	121.6(3)
C(2)–C(1)–C(7)	120.0(3)	C(2')–C(1')–C(7')	120.2(3)
C(3)–C(2)–C(1)	120.9(3)	C(3')–C(2')–C(1')	121.5(3)
O(3)–C(3)–C(2)	125.9(3)	O(3')–C(3')–C(2')	126.0(3)
O(3)–C(3)–C(4)	113.7(3)	O(3')–C(3')–C(4')	114.4(2)
C(2)–C(3)–C(4)	120.4(3)	C(2')–C(3')–C(4')	119.6(3)
O(2)–C(4)–C(5)	119.8(3)	O(2')–C(4')–C(5')	123.4(3)
O(2)–C(4)–C(3)	121.1(3)	O(2')–C(4')–C(3')	116.8(3)
C(5)–C(4)–C(3)	119.1(3)	C(5')–C(4')–C(3')	119.7(3)
C(4)–C(5)–C(6)	120.3(3)	C(4')–C(5')–C(6')	119.8(3)
C(1)–C(6)–C(5)	121.4(3)	C(1')–C(6')–C(5')	121.2(3)
C(1)–C(7)–C(8)	113.9(3)	C(1')–C(7')–C(8')	113.7(2)
C(9)–C(8)–C(7)	109.0(3)	C(9')–C(8')–C(7')	110.6(2)
C(9)–C(8)–C(8')	116.0(2)	C(9')–C(8')–C(8)	114.6(2)
C(7)–C(8)–C(8')	110.9(3)	C(7')–C(8')–C(8)	113.7(2)
O(1)–C(9)–C(8)	114.0(3)	O(1')–C(9')–C(8')	109.2(2)
C(3)–O(3)–C(10)	118.2(2)	C(3')–O(3')–C(10')	118.3(2)
Torsion angles / °			
C(9)–C(8)–C(8)–C(9)	33.2	C(4')–O(3')–C(3')–C(10')	–177.9
C(1)–C(7)–C(8)–C(8')	–70.1	O(2)–C(4)–C(3)–O(3)	0.7
C(1')–C(7')–C(8')–C(8)	–63.2	C(3)–C(4)–O(2)–H(2)	42.5
C(6)–C(1)–C(7)–C(8)	117.2	O(2')–C(4')–C(3')–O(3')	1.1
C(6')–C(1')–C(7')–C(8')	110.0	C(3')–C(4')–O(2')–H(2')	–162.8
C(4)–O(3)–C(3)–C(10)	175.2		

two phenyl rings are nearly parallel and almost faced at a distance of 3.53 Å: the dihedral angle between their planes is 4.7°, while the average angle between the line connecting the ring centers (distance X1 ··· X2 = 4.08 Å) and the normal to the rings is about 30°.

The analysis of bond distances and angles shows no abnormal value, but some interesting features are worth pointing out. There are some significant similarities and differences between the two halves of the molecule connected by the pseudo C_2 axis. Both phenyl rings have an alternating sequence of bond lengths, indicating the preference for one of the two Kekulé resonance forms (Figure 2) as a consequence of the substitution pattern. All torsion angles are as expected except for those around bond C8–C8'; indeed the value of the torsion angle C9–C8–C8'–C9' of 33.2° is quite narrow and far from the unstrained 60° value.

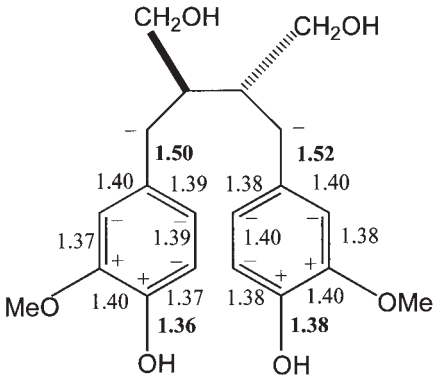

Figure 2. C–C distances and calculated charges in the vanillyl moieties in the crystal structure of (**1**).

An important factor in the stabilization of this geometry is the formation of a network of hydrogen bonds, the features of which are listed in Table IV and illustrated in Figure 3. The intramolecular hydrogen bond O1–H1 ··· O1' is probably a relevant factor in dictating the narrowing of the C9–C8–C8'–9' torsion angle. Both of the last two hydrogen bonds listed in Table IV involve oxygen O1', in the first acting as donor and in the second as acceptor. These two interactions link the two phenolic oxygens O2 and O2' of the same molecule with O1' of a neighboring molecule along the *c* axis. On the other hand, the strongest hydrogen bond O2'–H2' ··· O1 is almost parallel to the *b* axis. The intramolecular hydrogen bond and those involving the two phenolic groups are the driving forces for the facing of the two aromatic rings; indeed in iodophyllanthin,[13] where all hydroxyls are substituted by methoxy groups, the two phenyl rings, though parallel, do

TABLE IV

Hydrogen bonds (distances / Å, angles / deg)

H-bond	D ··· A	D–H	H ··· A	D–H ··· A	Symmetry operation
O(1)–H(1) ··· O(1')	2.689	0.99	1.81	146	
O(2')–H(2') ··· O(1)	2.663	0.85	1.82	170	x–1/2, –y+1/2, –z+2
O(2') ··· H(1')–O(1')	2.849	0.94	1.91	173	–x+3/2, –y, z+1/2
O(2)–H(2) ··· O(1')	2.892	0.85	2.05	169	–x+3/2, –y, z+1/2

D indicates the donor and A the acceptor.

not face each other. Formation of the intramolecular hydrogen bond O1–H1 ··· O1' is also responsible for the breaking of the C_2 symmetry, which was found in iodophyllanthin[13] and in the epoxylignan shonanin[14] (**2**), which have no hydroxyl groups in C9 and C9' and display an exact two-fold crystallographic symmetry. Shonanin must have the clustered conformation with the phenyl-phenyl facing because of the constraints imposed by the formation of the ether ring, forcing an eclipsed conformation around bond C8–C8'. In secoisolariciresinol (**1**), the formation of the intramolecular hydrogen bond between the synclinal hydroxymethyl groups in C8 and C8' imposes weaker constraints and also the intermolecular hydrogen bonds contribute to the clustering.

The small differences in bond distances between the two vanillyl moieties (Figure 2) are explained by their different involvement in hydrogen

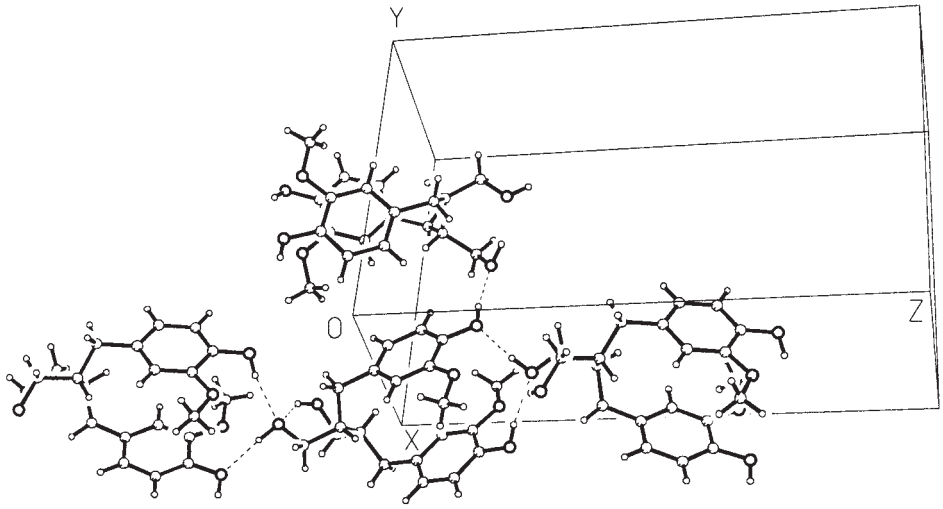

Figure 3. Crystal packing and hydrogen bonds in the crystal structure of (**1**).

bonds; indeed, while O2 acts as donor in only one weak bond, O2' is involved in two hydrogen bonds (a rather strong one where O2' acts as donor and a weaker one in which it acts as acceptor). In this way, in the first group a quinonic resonance form may be favored, while in the second the opposing effects of the two hydrogen bonds on O2' do not seem to affect the charge distribution of the ring.

Another interesting feature of the vanillyl groups is the narrowing of the O3–C3–C4 and O3'–C3'–C4' angles with a consequent decrease of the distance between the two negatively charged oxygen atoms. For the first moiety, the situation is in keeping with our findings on the related glycolate group,[15] indicating that the electrostatic repulsion between the negatively charged oxygen atoms is well counterbalanced by the interposed hydrogen, even when this is rotated by up to 60° to form an intermolecular hydrogen bond. In the second moiety, the O–H residue is rotated by more than 160° and its hydrogen is totally outside the region between the two oxygens, which are even closer because of the narrowing of also the C3'–C4'–O2' angle; nevertheless, the shielding effect is here realized by the interposition of atom H1' forming an intermolecular hydrogen bond with O2' and approaching O3' at a distance of 2.37 Å. A similar situation is found in (+ –)-methyltrachelogenin,[16] where all the phenolic hydroxyls are methylated.

In order to gain more insight into the molecular structure of secoisolariciresinol (**1**), we decided to carry out some *ab initio* calculations, with geometry optimization, on the three molecular systems illustrated in the scheme:

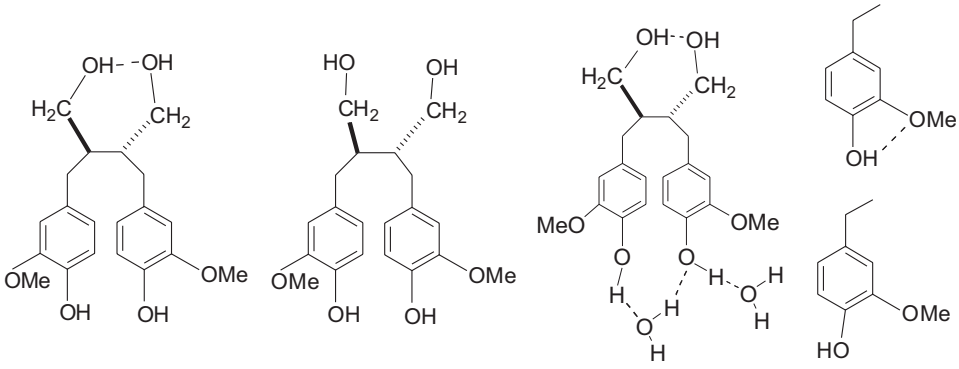

(**a**) the isolated molecule of (**1**) as in the crystal; (**b**) the same molecule without the intramolecular hydrogen bond; (**c**) the same molecule with two water molecules simulating the intermolecular hydrogen bonds; (**d**) a reduced

model with only one vanillyl moiety. The (**a**), (**b**), (**c**) geometries were optimized using the HF approximation with a mixed basis set: 6–31G(d,p) for hydrogens involved in hydrogen bonds and 6–31G(d) for all other atoms. The geometry of the smaller fragment (**d**) was optimized at the HF/6–31G(d,p) level. Single point DFT calculations were performed on the optimized geometries (**a**), (**b**) and (**d**) in order to better estimate their relative stability. A single point calculation, at the HF/6–31G(d,p) level, was also performed on the molecular geometry found in the crystal in order to obtain the corresponding electrostatic potential map.

All our calculations confirm that the phenyl rings of the vanillyl groups show the above mentioned preference for one of the two Kekulé resonance forms. The pattern of atomic charges indicates an electron depletion on both carbons linked to the oxygens and negative charges on C2 and C5, with a consequent lengthening of bond C3–C4 and shortening of bonds C2–C3 and C4–C5 (Figure 2). In the calculations on (**a**) and (**b**) all vanillyl groups have the same geometry, while in the crystal there are some small but significant differences between the two non-equivalent moieties, which can be ascribed to the intermolecular hydrogen bonds and to crystal packing effects. Unfortunately, the calculations on the simplified model of the hydrogen-bond pattern (**c**) cannot reveal such small differences.

Our calculations reproduce quite well the geometrical effects found in the crystal for the C10–O3–C3–C4–O2–H and C10'–O3'–C3'–C4'–O2'–H' regions, which have been previously described. Indeed, as in the crystal, the O2' $\cdots$ O3' = 2.59 Å distance is shorter than O2 $\cdots$ O3 = 2.69 Å and the angle C3'–C4'–O2' = 116.8 is considerably smaller than C3–C4–O2 = 121.3°. As in the case of the glycolate group,[15] there is an energy cost when the OH residue is rotated away from the inter-oxygen region; our Becke3LYP/6–311+G(2d,2p)//HF/6–31G(d,p) calculations on the two conformations of model (**d**) give a value of 4.3 kcal/mol for the energy of the repulsion between the two negatively charged oxygen atoms. The negative regions of the electrostatic potential (Figure 4), obtained from the calculations on the crystal geometry, indicate the acceptor ability of the different oxygen atoms. In Figure 4, it may be seen that there is a negative potential in the region between O2' and O3' confirming the electrostatic repulsion between these two atoms, which can only be overcome by the interposition of a hydrogen atom. The most negative regions of the electrostatic potential are found on O1 and O2', where the strongest hydrogen bonds are directed. The smaller negative regions near all other oxygen atoms indicate that they are less apt to behave as hydrogen-bond acceptors and, indeed, among them only O1' is involved in the weakest hydrogen bond.

In Table V, the values of the C9–C8–C8'–C9' torsion angle, as obtained from the calculations on different models, are reported with underneath the

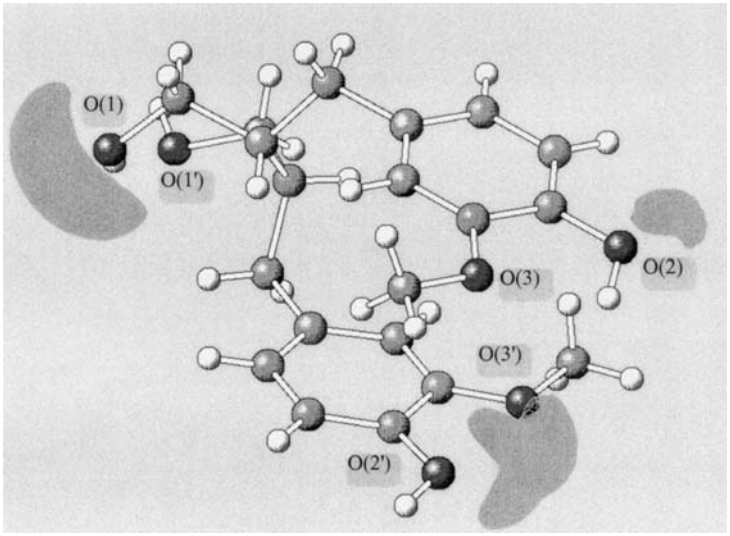

Figure 4. Negative regions of the electrostatic potential map as obtained from HF/6–31G(d,p) calculations on the crystal conformation of (**1**).

TABLE V

Values of the torsion angle C(9)–C(8)–C(8')–C(9') / deg in the crystal structure and after *ab initio* full geometry optimization of the different models

	Crystal	**a**	**b**	**c**	**c'**
C(9)–C(8)–C(8')–C(9')	33.2	44.6	61.2	41.2	40.7
Intramolecular H-bond	yes	yes	no	yes	yes
Intermolecular H-bonds	yes	no	no	yes	yes

In **c'** the geometry of the hydrogen-bond pattern is kept fixed as in the crystal.

indication of the presence or absence of intra- and/or inter-molecular hydrogen bonds. Comparison of the results of the calculations on (**a**) and (**b**) reveals the importance of the intramolecular hydrogen bond in dictating the clustered conformation. Indeed, the cost of breaking this hydrogen bond is estimated to be 5.1 kcal/mole at the Becke3LYP/6–31+G(d,p) level. Besides, in the optimum geometry of (**b**), the phenyl-phenyl facing is almost cancelled by the twist around the C8–C8' bond to reach the unstrained value of 60° of the torsion angle C9–C8–C8'–C9'. In macelignan,[17] where O1 and O1' are substituted by hydrogen atoms, no intramolecular hydrogen bond can be formed and the value of the torsion angle is 69.6°. The trend shown in Table V indicates that, besides the most relevant effect of the intramolecular hydrogen

bond (60 → 45°), also the intermolecular hydrogen bonds (45 → 41°) and the crystal packing (41 → 33°) contribute to the narrowing of the C9–C8–C8'–C9' torsion angle and to stabilization of the clustered conformation.

It is interesting to note that the full optimization of (**c**) yields almost the same results as that of (**c′**), where the hydrogen-bond pattern is kept fixed. Indeed, the optimized model (**c**) may be considered as a good simulation of the local effects of a polar solvent and its similarity with the hydrogen-bond pattern in the crystal allows us to infer that the molecule will assume the clustered conformation also in polar solvents.

Aknowledgments. – S.K.C and M.K. are grateful to the CIMAP director for providing the necessary facilities. M.M, D.V. and G.A. thank Professor P. Ugliengo and Dr. B. Civalleri for helpful discussions and acknowledge the financial support of MURST and CNR.

REFERENCES

1. K. Freudenberg and K. Weinges, *Tetrahedron Lett*. (1959) 19–23.
2. R. C. Powell and R. D. Plattner, *Phytochemistry* **15** (1976) 1963–1965
3. M. Schöttner, D. Ganßer, and G. Spiteller, *Planta Medica* **63** (1997) 529–532.
4. G. Traverso *Gazz. Chim. Ital*. **90** (1960) 792–807.
5. Siemens P3/PC Diffractometer Program, Version 3.13, Siemens Analytical X-Ray Instruments Inc., Madison, Wisconsin, U.S.A., 1989.
6. A. Altomare, G. Cascarano, C. Giacovazzo, A. Guagliardi, M. C. Burla, G. Polidori, and M. Camalli, *J. Appl. Crystallogr.* **27** (1994) 435–436.
7. G. M. Sheldrick, SHELXTL/IRIS, Siemens Analytical X-Ray Instruments Inc., Madison, Wisconsin, U.S.A., 1990.
8. G. M. Sheldrick, SHELXL-97, University of Göttingen, Germany, 1997.
9. M. J. Frisch, G. W. Trucks, H. B. Schlegel, P. M. W. Gill, B. G. Johnson, M. A. Robb, J. R. Cheeseman, T. Keith, G. A. Petersson, J. A. Montgomery, K. Raghavachari, M. A. Al-Laham, V. G. Zakrzewski, J. V. Ortiz, J. B. Foresman, J. Cioslowski, B. B. Stefanov, A. Nanayakkara, M. Challacombe, C. Y. Peng, P. Y. Ayala, W. Chen, M. W. Wong, J. L. Andres, E. S. Replogle, R. Gomperts, R. L. Martin, D. J. Fox, J. S. Binkley, D. J. Defrees, J. Baker; J. P. Stewart, M. Head-Gordon, C. Gonzalez, and J. A. Pople, *Gaussian 94, Revision C.3A.,* Gaussian, Inc., Pittsburgh PA, 1995.
10. W. J. Hehre, L. Radom, P. v. R. Schleyer, and J. A. Pople, *Ab initio molecular orbital theory*, 1st ed., John Wiley & Sons, New York, 1986, Chapter 4.
11. P. Ugliengo, D. Viterbo, and G. Chiari, *Z. Kristallog.* **207** (1993), 9–23.
12. F. H. Allen and O. Kennard, *Chemical Design Automation News* (1) **8** (1993) 1, 31.
13. J. A. Lerbscher, K. V. Krishna Rao, and J. Trotter, *Acta Cristallogr., Sect. B* **33** (1977) 1278–1284.
14. Jim-Min Fang, Kuo-Chio Hsu, and Yu-Shia Cheng, *Phytochemistry* **28** (1989) 3553–3558.
15. M. Milanesio, P. Ugliengo, D. Viterbo, and G. Appendino, *J. Med. Chem.* **42** (1999) 291–299.

16. K. Khamlach, R. Dhal, E. Brown, M. Leblanc, and G. Ferey, *Acta Cristallogr., Sect. C* **45** (1989) 1746–1750.
17. Won Sick Woo, Kuk Hyun Shin, H. Wagner, and H. Lotter, *Phytochemistry* **26** (1987) 1542–1548.

SAŽETAK

Kristalna i molekulska struktura sekoizolaricirezionola

Marco Milanesio, Davide Viterbo, Sunil K. Chattopadhyay, Manish Kulshrestha i Giovanni Appendino

Spoj *R,R*-2,3-bis[(4-hidroksi-3-metoksifenil)metil]-1,4-butandiol lignan sekoizolaricirezinol (**1**) sadržan je u gimnospermama, a primjenjuje se u terapiji dobroćudnih prostatičnih hiperplazija. U radu se izvješćuje o rezultatima kristalografskih i *ab initio* teorijskih istraživanja. Molekule spoja (**1**) u kristalima poprimaju klustersku konformaciju za koju je značajan međusobno usporedan i nasuprotan položaj dvaju fenilnih prstenova. Postojanost te geometrije postignuta je stvaranjem mreže vodikovih veza. Teorijski računi upućuju na to da je (*i*) unutarmolekulska vodikova veza O1–H1 ··· O1′ odlučujući čimbenik koji orijentira fenilne prstenove paraleno jedan naspram drugoga, dok međumolekulske vodikove veze kao i kristalno pakiranje u tome imaju manji učinak, (*ii*) da su nevezne interakcije 1–4O ··· O u vinilnim skupinama odlučujuće u određivanju najpostojanije konformacije i (*iii*) da proračuni s dvije eksplicitne kristalizacijske molekule vode u modelu dobro oponašaju lokalne učinke kristalizacijske vode i upućuju na to da (**1**) poprima vjerojatno klustersku konformaciju također i u polarnim otapalima.